JOURNAL OF MATERIALS SCIENCE 18 (1983) 365–374

Phase transformations in Ti–V alloys

Part 1 *Martensitic transformations*

E. SARATH KUMAR MENON*, R. KRISHNAN
Metallurgy Division, Bhabha Atomic Research Centre, Bombay, India-400 085

The morphology and substructure of the athermal martensite produced by β-quenching Ti, Ti–5% V and Ti–10% V have been described in detail. The martensitic transformation in the Ti–10% V alloy was found to be incomplete leading to a structure comprised of the α-, β- and ω-phases. The extent of β retention increases with the V content of the alloy and the martensitic transformation was completely inhibited on quenching a Ti–20% V alloy to room temperature. This alloy was found to undergo a stress-induced martensitic transformation. The morphology and crystallography of the stress-induced products have been examined in detail.

1. Introduction

Most of the commercial titanium alloys developed in the earlier days contained a high proportion of α stabilizers, e.g. Ti–8Al–1Mo–1V, Ti–6Al–4V, Ti–11Sn–2.25Al–5Zr–1Mo–0.25Si, Ti–4Al–2Sn–4Mo–0.5Si. Because of the lack of toughness in the solution-treated and aged condition and a relatively poor hardenability, these alloys have been used in the annealed condition and hence the strength capability has not been effectively utilized. However, recently, there has been a trend in producing many β alloys. The metastable β alloys possess processing advantages over the α–β alloys owing to the low elevated temperature flow stress. Because of the excellent hardenability and heat treatability of the β alloys (e.g. Ti–10V–2Fe–3Al, Ti–15V–3Cr–3Al–3Sn, Ti–13V–11Cr–3Al) this family would offer significant improvements in both strength and toughness with improved property uniformity throughout the forgings. It is significant that most of these newly developed metastable β alloys contain a relatively large addition of the β stabilizer, vanadium. Vanadium, though a weak β stabilizer, has the lowest density among the commercially used β-stabilizing elements like Mo, Cr, Fe, etc. Of course, owing to the low solid solution strengthening potency of V, strong solid solution strengtheners such as Fe, Cr, etc., are always present in the commercial alloys. A remarkable amount of strengthening can be brought about in these metastable β alloys by a judicious choice of proper heat treatments, thus producing suitable microstructural constituents distributed in a desirable manner.

In the work reported here and the following paper [1], different types of solid state phase transformations in some binary Ti–V alloys have been examined in detail with special emphasis on the characterization of the microstructures. In this paper, the morphology and substructure of two types of martensites, athermal martensite produced in Ti, Ti–5V and Ti–10V by β-quenching and stress-induced martensite in Ti–20V, have been described.

2. Experimental procedure

The alloys were prepared from sponge titanium and 99.99% pure vanadium granules by non-consummable arc melting. Chemical analysis of the alloys after homogenization at 1273 K for 24 h, showed their compositions to be Ti–4.93 wt% V, Ti–9.92 wt% V and Ti–20.06 wt% V. They will be referred to as Ti–5V, Ti–10V and Ti–20V, respectively, in the rest of the paper. The alloy ingots were encapsulated in evacuated mild

*Present address: Department of Metallurgical Engineering and Materials Science, Carnegie Mellon University, Pittsburgh, Pennsylvania 15213, USA.

0022–2461/83/020365–10$03.70/0

steel tubes and hot rolled in the temperature range 1073 to 1173 K to sheets of ~ 0.8 mm thickness. Specimens for all heat treatments were wrapped in tantalum foils and sealed in silica capsules under a protective atmosphere of helium at 175 mm pressure. All heat treatments were carried out in kanthal wound resistance furnaces and quenching was always done in ice-cold water.

Specimens for optical microscopy examination were etched in a solution containing 50 parts glycerol, 45 parts nitric acid and 5 parts hydrofluoric acid. Thin foils for transmission electron microscopy were prepared by the conventional window technique using an electrolyte containing 300 ml methanol, 165 ml *n*-butanol and 35 ml perchloric acid. The cathode was stainless steel and the electrolyte temperature was maintained below 220 K using a methanol-dry ice bath.

In order to study the stress-induced transformation in the Ti–20V alloy, tensile specimens having a gauge length of 12.5 mm were prepared from the rolled sheets. Tensile testing was carried out in a floor model Instron machine.

3. Results and discussion

3.1. Athermal martensite

A complete description of the structure of martensite essentially requires information regarding the crystal structure, the morphological appearance and the fine structure within the product phase.

3.1.1. Morphology

It has been observed in several alloy systems that the martensite structure is influenced to a great extent by alloy composition. Pure titanium and two of the alloys, namely, Ti–5V and Ti–10V were found to undergo the bcc to hcp transformation through a martensitic mode when quenched from the β-phase field. The martensitic product in the pure, unalloyed Ti samples showed the typical lath morphology (Fig. 1a) while the martensite produced in the Ti–10V alloy was found to possess a plate-type morphology (Fig. 1b). The structure of the Ti–5V alloy martensite could best be described as a mixed morophology. These observations are in agreement with the general nature of the martensite transformations in various Zr- and Ti-base alloys.

3.1.2. Crystal structure, orientation relationship and habit plane

X-ray diffraction analyses revealed that all these alloys consisted of a single hcp phase in the β-quenched condition. However, electron diffraction experiments showed that small quantities of the β-phase was present in the β-quenched Ti–10V alloy. The martensitic transformation was found to be incomplete and the parent β-phase persisted in the β-quenched Ti–10V alloy. This is best seen from the SAD pattern shown in Fig. 2 which clearly identifies the α- and the β-phases. The β regions contained some ω-phase, evidence for which was also obtained from the diffraction effects associated with the SAD patterns obtained from these regions (Fig. 3). It should be noted that the formation of the ω-phase during quenching was not possible in the Ti–5V alloy because, in this case, the M_s and the M_f temperatures are above the ω_s temperature [2]. However, for the Ti–10V alloy, M_s (very close to the ω_s) is very low and M_f is below room

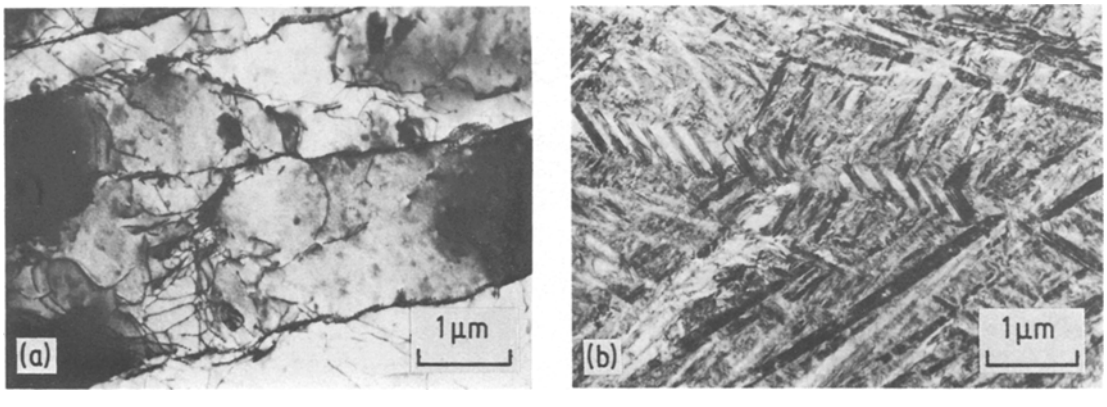

Figure 1 Typical appearance of the martensite formed on water quenching from the β-phase field in (a) Ti and (b) Ti–10V. The specimens were held at 1273 K for 15 min and subsequently water-quenched.

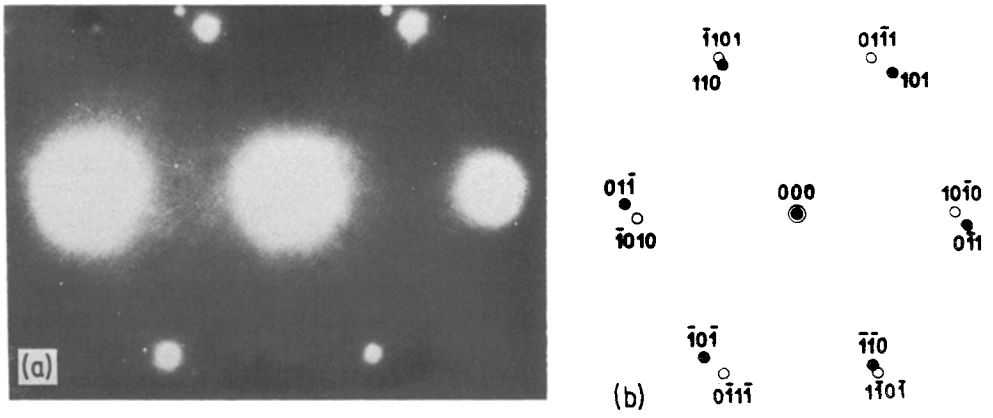

Figure 2 (a) SAD pattern showing the presence of both the α and the β reflections. Zone axes: $[111]_\beta$ and $[1\bar{2}13]_\alpha$. (b) Key to (a).

temperature [2], and hence the $\beta \rightarrow \alpha'$ martensitic transformation does not go to completion and the $\beta \rightarrow \omega$ transformation occurs. The co-existence of the α'-, β- and ω-phases in the β-quenched Ti–10V alloy noticed in the present work appears to be qualitatively similar to the results reported by Collings [3] from magnetic susceptibility measurements.

The orientation relationship observed in all these alloys was found to be the same as that described by Burgers [4]. Habit-plane determination showed that the martensite always possessed a near $\{1\,1\,1\}_\beta$ habit. An unambiguous habit-plane solution could not be obtained as there was a lot of scatter in the data and it is very difficult to distinguish the $\{3\,3\,4\}_\beta$ and the $\{3\,3\,4\}_\beta$ habits which are the normally observed habits in Zr and Ti martensites [6–8], as the {334} and the {344} poles lie close to the {111} pole. A similar observation has been made in Zr-base alloy martensites earlier [9].

3.1.3. Substructure of the product phase

A typical example of the internal structures of the martensite laths is shown in Fig. 4a. Adjacent laths were found to be separated by small-angle boundaries (Fig. 4b). The laths in the Ti–5V alloy were considerably smaller in size and the dislocation content was much higher in comparison to the martensite units in unalloyed titanium. The simultaneous presence of laths and plates of martensite has been reported in several alloys and this is believed to be associated with an intermediate M_s temperature [9–11]. The martensite plates in the Ti–5V alloy were observed to be twin-free (Fig. 4c) while the plates in the Ti–10V alloy were heavily twinned (Fig. 4d). Of course, it must be pointed out that not all the martensite plates were observed to be twinned in the Ti–10V alloy samples studied here. The β-quenched specimens were found to be partitioned by large primary plates which are formed in the initial stages of the transformation, the intervening regions being occupied by smaller secondary plates belonging to later generations. Many, if not all, of the primary plates were internally twinned, while twinning within the secondary plates was infrequent. The twins were found to be predominantly of the $\{10\bar{1}1\}_\alpha$ type. Williams *et al.* [12] have suggested that the twins in the primary plates are generated due to post-transformation shear. They have pointed out that if twinning is to be produced by a component of the transformation shear, the the twin formation would be more favourable in the secondary plates which are formed at temperatures lower than those corresponding to the

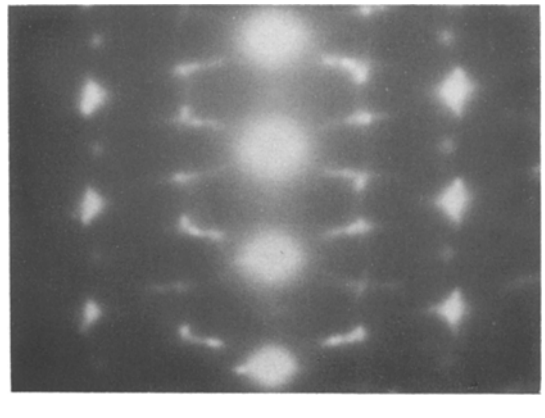

Figure 3 SAD pattern illustrating the diffuse scattering associated with the ω-phase. Zone axis: $[1\,1\,3]_\beta$.

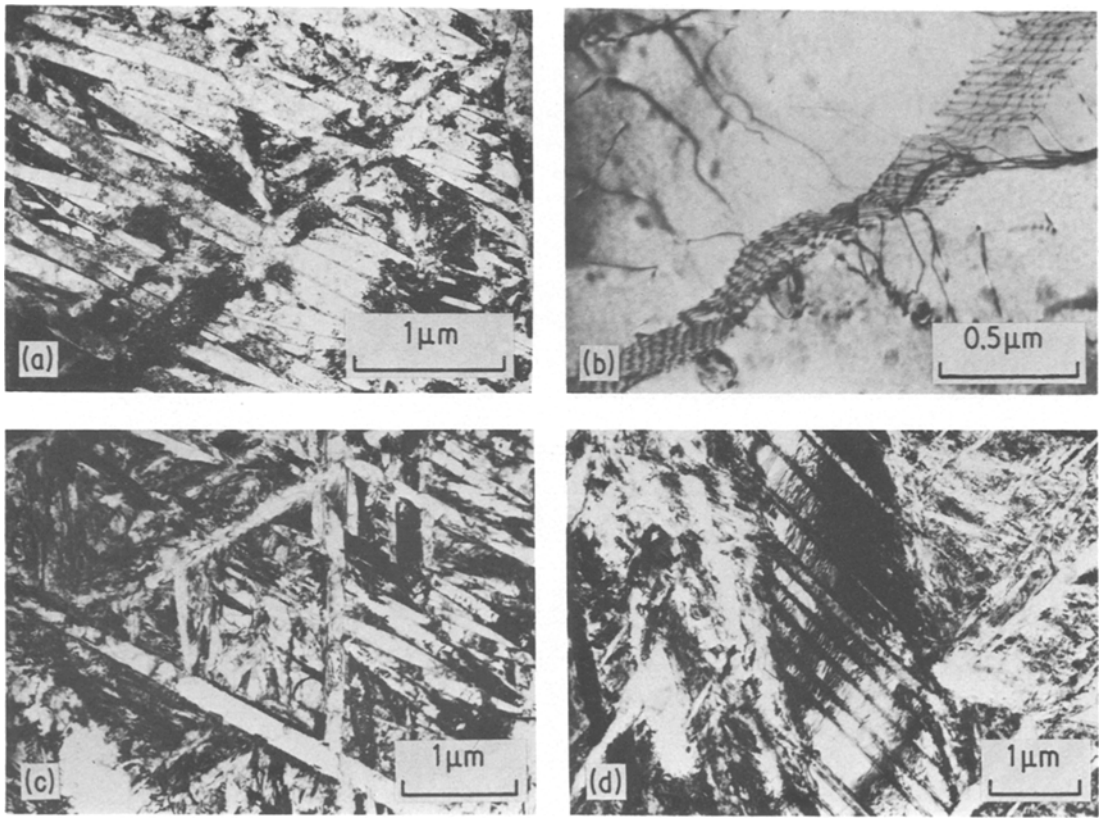

Figure 4 Substructure of the martensites. (a) Heavily dislocated laths in Ti–5V. (b) Lath boundary in Ti. (c) Twin-free plates in Ti–5V. (d) Internally twinned primary martensite plate in Ti–10V.

primary plates. In the present work, however, the occurrence of almost equi-spaced twins of nearly identical thickness in many plates suggested that these are transformation twins. Furthermore, the internal twinning of the primary plates did not appear to result from secondary plate impingement. A similar observation has also been made earlier in various zirconium-base alloys [10, 13, 14]. In many instances, the twin bands in the primary plates showed a regular distribution of dislocations aligned in parallel arrays (Fig. 4d). Similar arrangements of dislocations were noticed very frequently and trace analyses indicated that these dislocations were on the $\{10\bar{1}1\}_\alpha$ planes. This observation, showing a uniform distribution of dislocations, suggested that an inhomogeneous shear occurred by slip on the $(01\bar{1}1)_\alpha$ even within the $(10\bar{1}1)_\alpha$ twin bands. The implication of this is that the total inhomogeneous shear is made up of two parts, one operating on $(10\bar{1}1)_\alpha$ and the other on the $(01\bar{1}1)_\alpha$ through a twin mode and a slip mode, respectively. Slip along the $\{10\bar{1}1\}_\alpha$ could occur in either the $\langle 11\bar{2}3\rangle_\alpha$ or in the $\langle 1\bar{2}10\rangle_\alpha$ by the movement of the dislocations with Burgers vectors of the type $1/3\langle 11\bar{2}3\rangle_\alpha$ (i.e. $\langle \mathbf{c}+\mathbf{a}\rangle$ type) and $1/3\langle 1\bar{2}10\rangle_\alpha$ (i.e., $\langle \mathbf{a}\rangle$ type), respectively [15]. Contrast experiments revealed that the dislocations left behind as the debris of slip on the $(01\bar{1}1)_\alpha$ was of the $\langle \mathbf{c}+\mathbf{a}\rangle$ type indicating that multiple shear was composed of $(10\bar{1}1)_\alpha$ twin shear and a $(01\bar{1}1)$ $[11\bar{2}\bar{3}]$ slip shear. The two components of this multiple shear are mutually compatible since the direction of the second shear, $[11\bar{2}\bar{3}]_\alpha$, is parallel to the plane of the first shear, $(10\bar{1}1)_\alpha$.

In addition to the $\{10\bar{1}1\}_\alpha$ twins, primary martensite plates contained features which appeared to be similar to stacking faults (Fig. 5). These features were found to lie on the $\{10\bar{1}1\}_\alpha$ planes. Visibility criteria could not be established owing to overlapping fault images. Similar features have been reported earlier in Zr–Ti alloys containing O_2 or Mo [16] and also in Ti–Cr alloys.

3.2. Stress-induced martensite

A great deal of attention has recently been focused

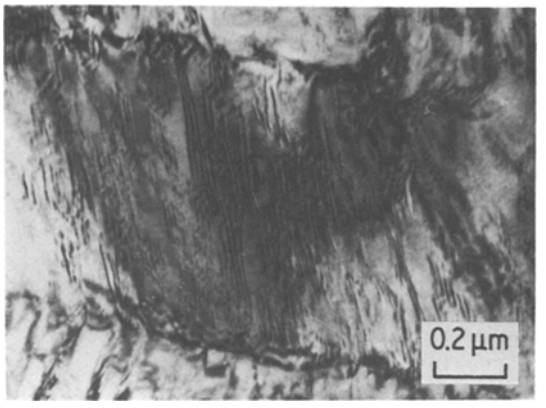

Figure 5 Ti–10V, β-quenched. Bright-field micrograph illustrating the stacking faults within a martensite plate.

on the formation of martensite in β titanium alloys during stressing. Furthermore, considerable controversy has arised in connection with this subject because of conflicting evidence regarding the nature of the stress-induced products. Some have conclusively shown that no new phase is produced during deformation [18–20], while others have observed the presence of stress-induced martensite [21–26]. It appears that alloy chemistry plays an important role in determining whether the stress-induced product in a given alloy is deformation twinning or stress-induced martensite. The confusion arises because light microscopy alone is insufficient to identify the product since both twins and the martensite have the same appearance as was pointed out by Williams [24]. Again, there is a great deal of disparity in the literature regarding the crystal structure of the stress-induced product [20, 21, 27, 28] although according to Williams [24], the stress-induced product in titanium alloys has invariably an orthorhombic crystal structure. The detection of the orthorhombic phase by X-ray diffraction is relatively simple since its characteristic pattern has five low-angle peaks compared to the three peaks for the hexagonal close-packed martensite. However, sometimes, depending on the alloy content, an insufficient separation between the low-angle lines (1 1 0) and (0 2 0), and the (0 2 1) and (1 1 1), makes the differentiation between the orthorhombic and the hcp structures very difficult.

3.2.1. Metallographic observations

The high-temperature β-phase was found to be retained in the quenched Ti–20V specimens and metallographic examinations showed the presence of equiaxed β grains. In contrast, the microstructure of the tensile-tested specimens was characterized by plate-like features fragmenting the β grains (Fig. 6a). It was always noticed that the stress-induced transformation was confined to the gauge length of the tensile specimens and that the microstructure near the gripped end of the specimens were exactly identical to that of the as-quenched specimens. The stress-induced plates were frequently found to have an internal substructure (Fig. 6b). This structure was very similar to the internal structure of martensite plates.

3.2.2. X-ray diffraction

X-ray diffraction of the β-quenched Ti–20V samples showed the presence of only bcc reflections. However, X-ray diffraction patterns obtained

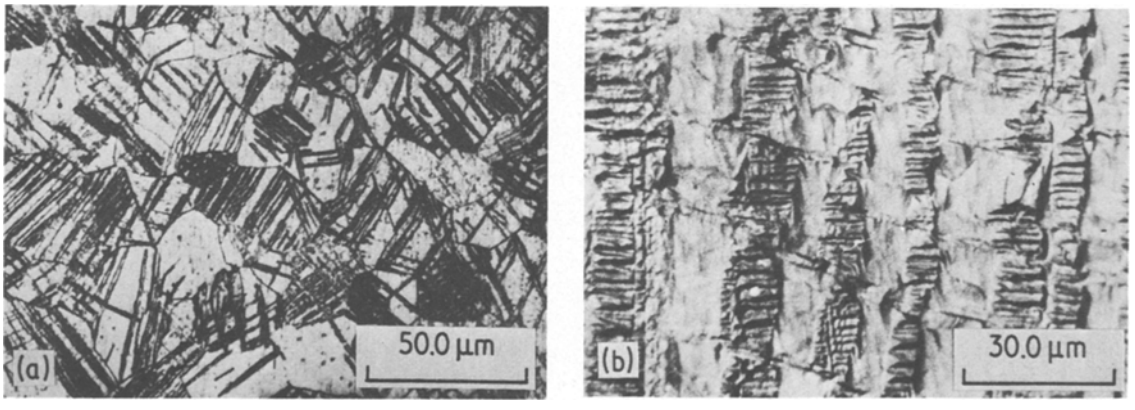

Figure 6 Ti–20V, β-quenched and fractured in uniaxial tension. (a) Optical micrograph showing the typical appearance of the stress-induced products. (b) Optical micrograph illustrating the internal features associated with the stress-induced products.

from the deformed specimens were characterized by five lines on the low-angle side of the diffractometer chart. From the diffraction data (Table I), it was possible to identify the structure of the stress-induced product as base-centred orthorhombic, isostructural with the A-20 (α-uranium) structure. The unit cell dimensions of the orthorhombic phase were found to be $a = 0.2589$ nm; $b = 0.4200$ nm and $c = 0.3838$ nm. The presence of stress-induced martensite in binary Ti–V alloys have not been reported so far, but deformation induced martensite in various titanium alloys has been found to possess an orthorhombic structure [23, 24, 26]. The orthorhombic structure is a highly distorted form of the hcp structure and many titanium-base alloys are known to produce an orthorhombic martensite on β-quenching [24, 29, 30]. The mechanism of this bcc to orthorhombic transformation was discussed in detail by Duerig *et al.* [26, 31].

3.2.3. Transmission electron microscopy observations

TEM investigations have revealed the morphological and crystallographic details of the stress-induced products. SAD patterns obtained solely from these plate-shaped features could be indexed only as a superposition of the reciprocal lattice sections of the bcc and the orthorhombic phases. An example is shown in Fig. 7. The SAD pattern obtained from the region marked A in Fig. 7a is shown in Fig. 7b and the key to this pattern is shown in Fig. 7c. It can be ssen from Fig. 7b and c that the orthorhombic phase is twinned on the (2 1 1) planes. Usually, orthorhombic martensites in titanium alloys are found to twin on the (1 1 1) planes [24]. However, Oka *et al.* [32] have observed twinning on the (1 1 0), (1 0 1) and (0 1 1) planes in the orthorhombic martensite in a Ti–12.6%V alloy. In this context, it is pertinent to point out that an orthorhombic structure can twin on a variety of planes as shown by Crocker [33], including the (2 1 1) planes. The habit plane of the orthorhombic martensite was found to be very close to the $\{1\,3\,3\}_\beta$. The orthorhombic martensite produced in Cu–Al alloys has been reported [34, 35] to possess a $(1\,3\,3)_\beta$ habit which is the predicted habit plane in the bcc to orthorhombic martensite transformation.

TABLE I X-ray data for the orthorhombic phase

hkl	*d*-spacing (nm)	
	Observed	Calculated*
1 1 0	0.2281	0.2205
0 2 0	0.2094	0.2101
0 0 2	0.1926	0.1919
1 1 1	0.1910	0.1912
0 2 1	0.1873	0.1843
1 1 2	0.1441	0.1448
0 2 2	0.1421	0.1417
2 0 0	0.1296	0.1295
1 3 1	0.1154	0.1173

*On the basis of $a = 0.2589 \pm 0.004$ nm; $b = 0.4203 \pm 0.0007$ nm and $c = 0.3838 \pm 0.006$ nm.

Microstructural investigations have revealed that the stress-induced transformation could be totally suppressed by ageing the β-quenched alloy in the $(\alpha + \beta)$ phase field. It was noticed that while stress-induced products formed during deformation of the samples aged at 823 K for 10 min, no plate-like features were present in samples aged at 823 K for 100 and 1000 min. This can be attributed to the enrichment of the β-phase with V as a result of α precipitation during ageing which subsequently led to the stabilization of the matrix with respect to the stress-induced transformation. In this context, it is pertinent to recall the observations of Paris *et al.* [37] who have noted a transition in the deformation mode from twin to slip in β-quenched Ti–20V alloy subjected to sequentially longer ageing treatments in the two-phase field. They also showed that twinning predominates only when the V content is less than 24%. These considerations suggest that there is a close relationship between the mode of deformation and the formation of the orthorhombic stress-induced martensite.

3.2.4. Observation of $\{1\,5\,3\}_\beta$ twinning

The SAD pattern shown in Fig. 8a was obtained from the region marked C in Fig. 7a and shows that the matrix bcc crystal and the bcc crystal in the stress-induced plate are related through an unusual mode of twinning. The relative orientations of the two bcc crystals are represented in the stereogram shown in Fig. 8c. Twinning along the {1 5 3} planes of the bcc structure is unusual. Richman [38] has pointed out that bcc materials which deform primarily by mechanical twinning exhibit unusual twin habits such as {0 1 3}, {0 8 9} and {1 2 7}. It should be mentioned that apart from {1 5 3} twinning, {1 1 2} twins were also observed in deformed Ti–20V specimens. Again, unusual twin habits such as {3 3 2} and {2, 4.8, 4.8} have been reported to form during deformation in

metastable β titanium alloys containing quenched-in ω particles [19, 23, 39]. According to Blackburn and Feeney [23], shears associated with {3 3 2} twinning are compatible with the ω structure whereas those attendant with {1 1 2} are not. Although it is reported that two {1 1 2} twins can interact to form a ⟨1 5 3⟩ intersection [40], the type of relation observed in the present work has not been reported.

In this context, it appears necessary to point out that a certain amount of caution has to be excercised before an unambiguous identification of the twinning system is made. This in indeed very important in the case cited here especially when one finds that a crystal in ⟨1 1 1⟩ orientation can change to ⟨1 1 3⟩ orientation also by {3 3 2} twinning [41]. This calculation is very easily performed using the general method described by Johari and Thomas [42]. It is found that a crystal in ⟨1 1 1⟩ orientation can change to ⟨7 5 17⟩, ⟨5 13 13⟩ or ⟨1 1 17⟩ orientations by {3 3 2} twinning whereas by {1 5 3} twinning, it can change to ⟨17 19 55⟩, ⟨1 5 7⟩, ⟨37 25 41⟩ or ⟨25 5 53⟩ orientations. It is to be noted that ⟨7 5 17⟩ and ⟨17 19 55⟩ are 4.5° and 1.4°, respectively, from ⟨1 1 3⟩. However, if one were to look at the SAD patterns taken from the matrix and the twinned crystals, the two types of twinning can be easily distinguished as the two reciprocal lattice sections corresponding to the different twinned crystals, though of identical zone axis, are rotated by about 17.5° with respect to the matrix pattern. This is easily seen from a comparison of Fig. 8b with Fig. 9. Thus it is conclusively determined that the twin relation observed here is {1 5 3} twinning and not of the {3 3 2} type.

4. Conclusions

(1) The morphology of the martensite produced in Ti can be drastically changed by alloying. The morphology changes from dislocated lath to internally twinned plate with increasing V content.

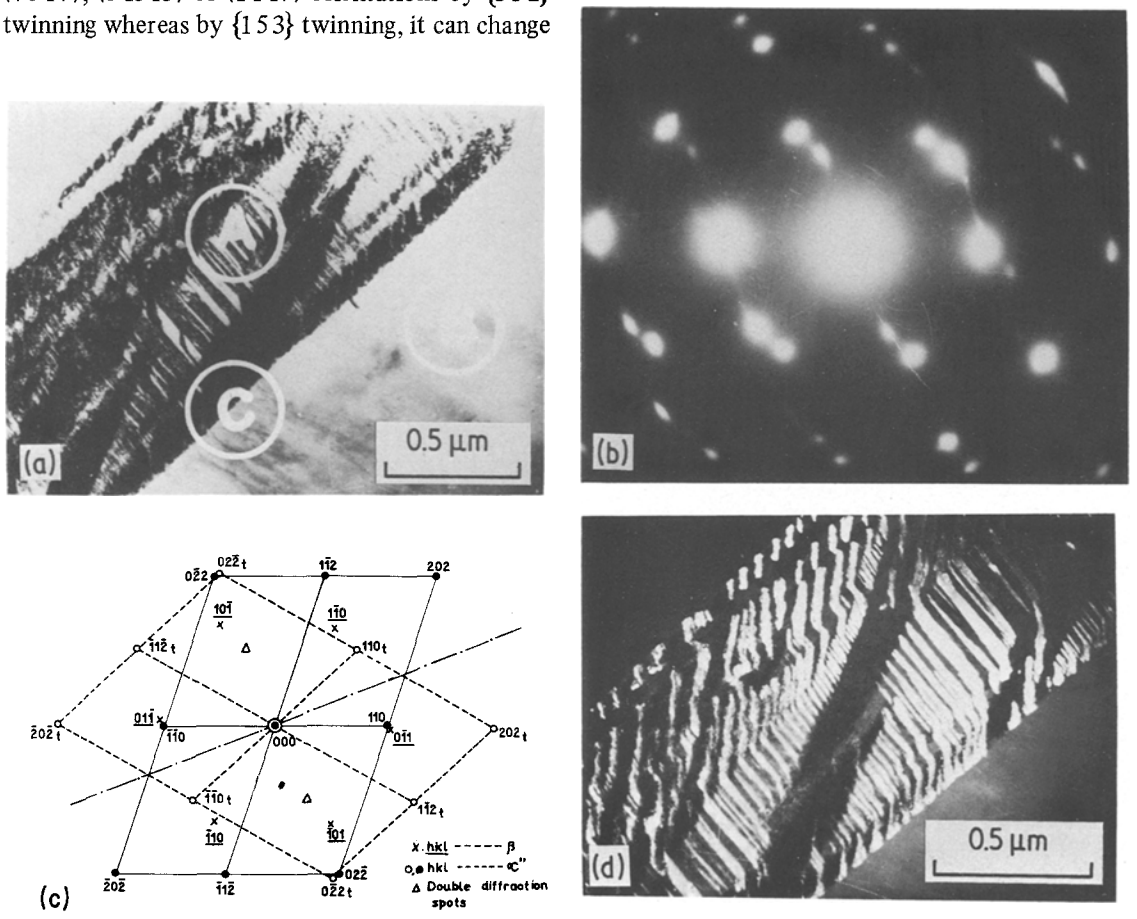

Figure 7 Ti–20V alloy, β-quenched and tensile-tested at room temperature. (a) Bright-field micrograph showing the morphology and internal structure of a stress-induced plate. (b) SAD pattern, and (c) key. (d) Dark-field micrograph obtained from the spot marked $(1\,1\,0)_t$.

Figure 8 SAD pattern obtained from the region marked C in Fig. 7a, and (b) key. (c) Stereogram illustrating the relative orientations of the matrix and the twinned b c c crystals, respectively.

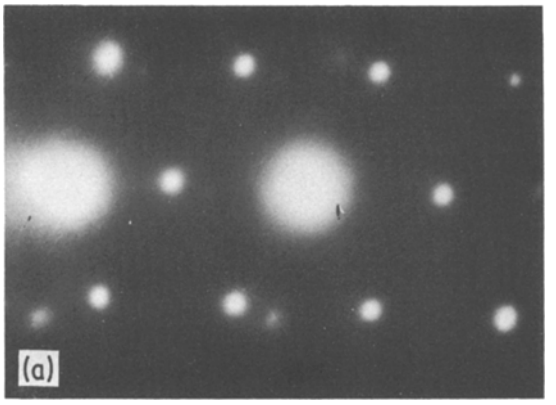

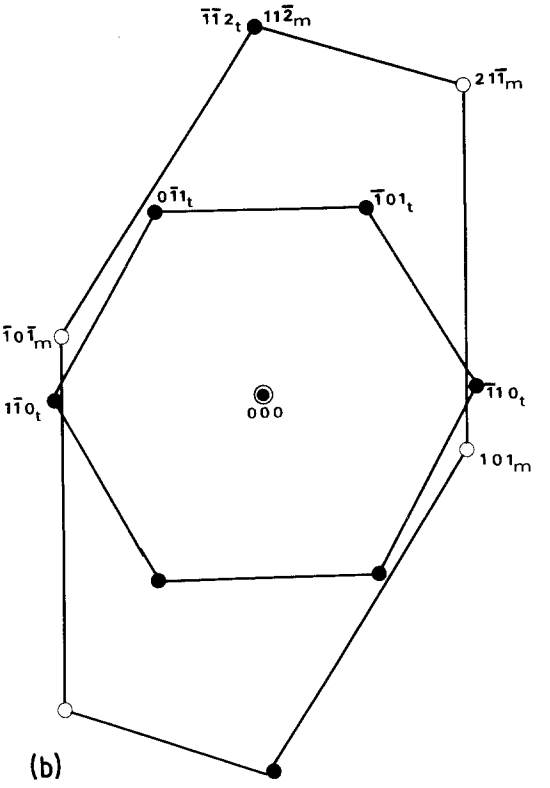

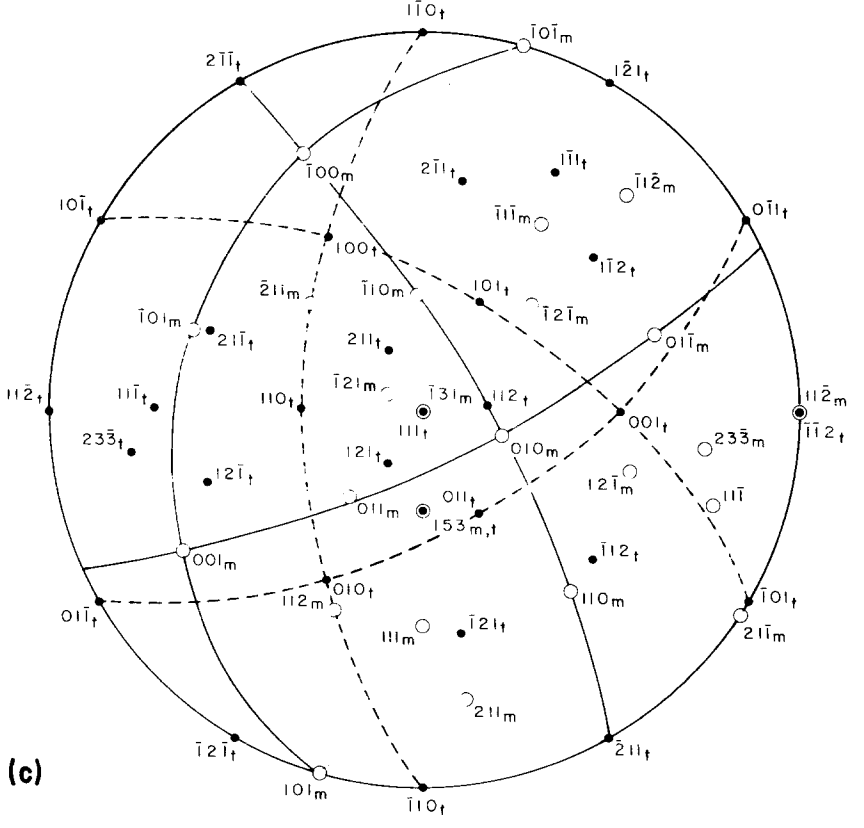

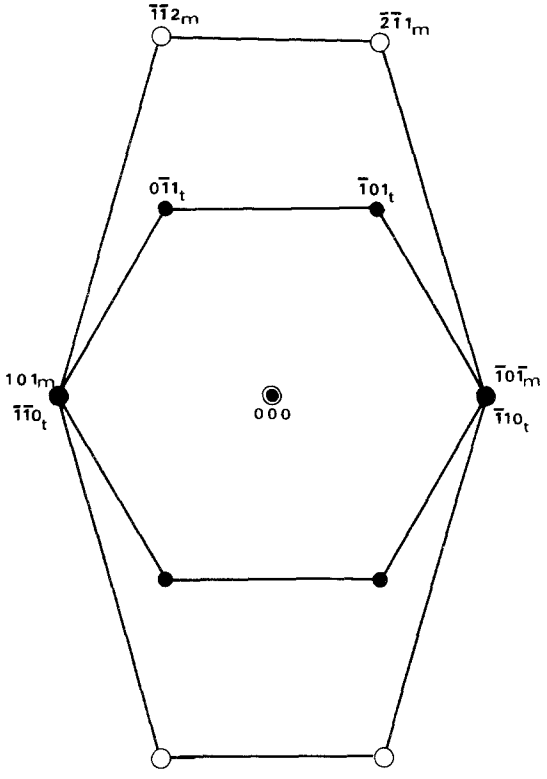

Figure 9 Calculated SAD pattern showing the relative orientations of the matrix and the $(23\bar{3})$ twinned bcc crystal. Note that the zone axes are the same as those in Fig. 8b but the twin pattern is rotated by ~ 17.5°.

(2) The plate martensite showed predominantly $\{10\bar{1}1\}_\alpha$ twinning. It was also noticed that two lattice invariant shears operated in the plate martensite formation. Also, in addition to twins and dislocations, faults were noticed in the Ti–10V alloy martensite.

(3) The martensitic transformation in the Ti–10V alloy was found to be incomplete in the sense that some amount of the β-phase, together with the ω-phase, was noticed in the β-quenched specimens.

(4) The Ti–20V alloy, in which the high-temperature β-phase was retained in a metastable manner on quenching, was found to undergo a stress-induced martensitic transformation. The stress-induced martensite possesses an orthorhombic crystal structure and was found to twin on the (2 1 1) planes.

(5) The β-phase showed an unusual twinning mode, {1 5 3}, during deformation apart from the usual {1 1 2} twinning.

5. Acknowledgements

The authors wish to thank Drs M. K. Asundi, P. Mukhopadhyay and Messrs M. Sundararaman, J. K. Chakravartty and S. L. Wadekar for many useful discussions and help during different stages of this work.

References

1. E. S. K. MENON and R. KRISHNAN, *J. Mater. Sci.* **18** (1983) 375.
2. P. DUWEZ, *Trans. ASM* **45** (1953) 934.
3. E. W. COLLINGS, *J. Less-Common Metals* **39** (1975) 63.
4. W. G. BURGERS, *Physica* **1** (1934) 561.
5. J. W. CHRISTIAN, "The Mechanism of Phase Transformations in Crystalline Solids" (Institute of Metals, London, 1969) p. 129.
6. Y. C. LIU, *Trans. AIME* **206** (1956) 1036.
7. C. HAMMOND and P. M. KELLY, in "The Science, Technology and Applications of Titanium", edited by R. I. Jafee and N. E. Promisel (Pergamon Press, Oxford, 1970) p. 659.
8. P. GAUNT and J. W. CHRISTIAN, *Acta Metall.* **7** (1959) 534.
9. S. BANERJEE, PhD thesis, Indian Institute of Technology, Kharagpur, India (1973).
10. S. BANERJEE and R. KRISHNAN, *Met. Trans.* **4** (1973) 1811.
11. S. BANERJEE, S. J. VIJAYAKAR and R. KRISHNAN, in "Titanium Science and Technology", Vol. 3, edited by R. I. Jaffee and H. M. Burte (Plenum Press, New York, 1973) p. 1597.
12. J. C. WILLIAMS, R. TAGGART and D. H. POLONIS, *Met. Trans.* **1** (1970) 2265.
13. S. BANERJEE and R. KRISHNAN, *Acta Metall.* **19** (1971) 1317.
14. P. MUKHOPADYAY, E. S. K. MENON, S. BANERJEE and R. KRISHNAN, *Z. Metallkde* **69** (1978) 728.
15. P. G. PARTRIDGE, *Met. Rev.* **118** (1967) 169.
16. H. M. FLOWER and P. R. SWAN, in "Titanium Science and Technology", Vol. 3, edited by R. I. Jaffee and H. M. Burte (Plenum Press, New York, 1973) p. 1507.
17. R. H. ERICKSON, R. TAGART and D. H. POLONIS, *Acta Metall.* **17** (1969) 553.
18. H. J. RACK, D. KALISH and K. D. FIKE, *Mater. Sci. Eng.* **6** (1970) 181.
19. M. OKA and Y. TANIGUCHI, *Met. Trans.* **10A** (1979) 651.
20. J. A. FEENEY and M. J. BLACKBURN, *ibid.* **1** (1970) 3309.
21. R. A. WOOD, D. N. WILLIAMS, J. D. BOYD, R. L. ROTHMAN and E. S. BARTLETT, AFML-TR-70-257 (1970).
22. M. J. BLACKBURN and J. C. WILLIAMS, *Trans. AIME.* **242** (1968) 2461.
23. M. J. BLACKBURN and J. A. FEENEY, *J. Inst. Metals* **99** (1971) 132.
24. J. C. WILLIAMS, in "Titanium Science and Technology", Vol. 3 edited by R. I. Jaffee and H. M. Burte (Plenum Press, New York, 1973) p. 1433.
25. N. E. PATON and J. C. WILLIAMS, Proceedings

of Conference on Strengths on Metals and Alloys, Asilomer, ASM (1971) p. 108.
26. T. W. DUERIG, G. T. TERLINDE and J. C. WILLIAMS, *Met. Trans.* **11A** (1980) 1987.
27. M. K. KOUL and J. F. BREEDIS, *Acta Metall.* **18** (1970) 579.
28. T. S. KUAN, R. R. AHRENS and S. L. SASS, *Met. Trans.* **6A** (1975) 1767.
29. A. R. G. BROWN, D. CLARK, J. S. ESTABROOK and K. S. JEPSON, *Nature*, **201** (1964) 914.
30. J. C. WILLIAMS and B. S. HICKMAN, *Met. Trans.* **1** (1970) 2648.
31. T. W. DUERIG, R. M. MIDDLETON, G. T. TERLINDE and J. C. WILLIAMS, in "Titanium '80", Vol. 2, edited by H. Kimura and O. Izumi, (AIME, 1980) p. 1503.
32. M. OKA, C. S. LEE and K. SHIMIZA, *Met. Trans.* **3** (1972) 37.
33. A. J. CROCKER, *J. Nucl. Mater.* **16** (1965) 306.
34. A. G. GRENINGER, *Trans. AIME.* **133** (1939) 204.
35. P. R. SWAN and H. WARLIMONT, *Acta Metall.* **11** (1963) 511.
36. J. W. CHRISTIAN, "Theory of Transformations in Metals and Alloys", (Pergamon Press, Oxford, 1965).
37. H. G. PARIS, B. G. LEFEVRE and E. A. STARKE, Jr, *Met. Trans.* **7A** (1976) 273.
38. R. H. RICHMAN, in "Deformation twinning", edited by R. E. Reed-Hill, J. P. Hirth and H. C. Rogers (Gordon and Breach, New York, 1962) p. 237.
39. J. A. ROBERSON, S. FUJISHIRO, V. S. ARUNACHALAM and C. M. SARGENT, *Met. Trans.* **5** (1974) 2317.
40. S. MAHAJAN, *ibid.* **12A** (1981) 379.
41. M. HIDA, E. SUKEDAI, Y. YOKOHARI and A. NAGAKAWA, *J. Jap. Inst. Metals* **4** (1980) 436.
42. O. JOHARI and G. THOMAS, *Trans. AIME* **230** (1964) 597.

Received 18 January
and accepted 24 June 1982